Performance Evaluation Of Reconfigurable Intelligent Surface Aided Multi-Hop Relaying Schemes With Short Packet Communication

Pham Minh QUANG[1], *Nguyen Trong KIEN*[1], *Tran Trung DUY*[1], *Ngo Hoang AN*[2,3], *Nguyen Tien TUNG*[2], *Anh-Vu LE*[4]

[1]Posts and Telecommunications Institute of Technology Ho Chi Minh City, Vietnam
[2]Faculty of Electronics Technology, Industrial University of Ho Chi Minh City (IUH), Ho Chi Minh City 700000, Viet Nam
[3]Ho Chi Minh City University of Industry and Trade, Ho Chi Minh City, Vietnam
[4]Communication and Signal Processing Research Group, Faculty of Electrical and Electronics Engineering, Ton Duc Thang University, Ho Chi Minh City, Vietnam

quangpm@ptit.edu.vn, ntkien@ptit.edu.vn, duytt@ptit.edu.vn, annh@huit.edu.vn, nguyentientung@iuh.edu.vn, leanhvu@tdtu.edu.vn

DOI: 10.15598/aeee.v22i1.5583

Article history: Received Dec 06, 2023; Revised Feb 19, 2024; Accepted Mar 23, 2024; Published Mar 31, 2024.

Abstract. *This paper proposes and studies performance of reconfigurable intelligent surface (RIS)-assisted multi-hop schemes employing short packet communication (SPC). In the proposed schemes, a source sends its data to a destination, and one RIS is deployed to assist the data transmission at each hop. For complexity reduction purposes, we propose two RIS-assisted data transmission methods at each hop. In the first one, the RIS is only used when the quality of the direct link is not good. In the second one, the direct link or the relay link via the RIS is selected for the data transmission. We evaluate performance of the two proposed schemes by deriving formulas of end-to-end block error rate (BLER-e2e) over Rayleigh fading channel. Finally, the derived BLER-e2e expressions are validated by computer simulations.*

Keywords

Intelligent reflecting surface, short packet communication, multi-hop relaying, cooperative communication.

1. Introduction

Relaying techniques [1–13] are often applied to wireless communication networks to improve network performance under the impact of fading channels. In [1,2], intermediate nodes within radio range of both source and destination nodes (called relay nodes) are employed to assist in source-to-destination data transmission. In [3], multi-hop schemes using multiple relays are studied because the destination is far from the source. In [4], route selection algorithms are applied for multi-hop multi-path wireless sensor networks, where sensor nodes, whose transceiver hardware is imperfect, have to harvest energy from radio signals for data transmission. Moreover, the published work [4] considers the presence of active eavesdroppers, and therefore, sensor nodes have to reduce their transmit power to protect the source data. In [5], a multi-hop network using full-duplex relaying techniques and operating in a near-field path-loss environment is proposed and evaluated. Additionally, the authors in [5] consider non-orthogonal multiple access techniques and the issue of imperfect interference cancellation. Published works [6–13] introduce various practical applications of the relaying techniques in wireless communication networks.

Recently, relaying networks that use reconfigurable intelligent surfaces (RIS) have been studied. Unlike the conventional relaying methods, in [14–18], the RIS, which consists of a lot of small reflectors, is deployed to optimally reflect the source signals to the desired destination. In particular, the RIS uses controllers to appropriately adjust the phases of the radio waves so that they can be reflected to the destination optimally. In [19], the authors study secrecy performance for a down-link relaying scenario using the RIS. As in [19], the RIS-aided scenario obtains better performance than the corresponding one using the conventional relays. In [20], the authors analyze average secrecy capacity of secure transmission relaying models using the RIS with discrete phase shift. The authors in [21] investigate secrecy performance of RIS-assisted vehicle-to-vehicle and vehicle-to-infrastructure networks.

Short packet communication (SPC) has garnered a lot of attention of researchers for its applications in ultra-reliable low-latency communication networks. In [22], the authors propose and optimize block error rate (BLER) performance of dual-hop relaying schemes employing SPC. Published works [23, 24] study cluster-based multi-hop relaying models utilizing SPC, and incorporating relay selection at each hop. Notably, the transmitting nodes in these models are required to harvest wireless energy from power stations. In [25], the authors assessed BLER performance of dual-hop underlay cognitive radio networks with the assistance of the RIS.

In this paper, we propose the RIS-aided multi-hop scheme using SPC. In particular, the RIS is employed to assist the data transmission at each hop on the source-to-destination route. Although published works [26, 27] also study multi-hop networks using hop-by-hop cooperative transmission, [26, 27] do not consider the SPC and RIS techniques. In contrast to [28–33], this paper considers the multi-hop relaying networks, while these published works consider RIS-aided dual-hop networks. In [34], the authors evaluate outage performance of the RIS-aided multi-hop networks, but they] do not study the SPC technique.

Next, this paper briefly introduces motivation, new points and main contributions:

- We propose two new RIS-aided hop-by-hop transmission methods for the proposed scheme. In the first one (named RIS-IC), Incremental Cooperation strategy is applied at each hop, where the RIS is only used if the direct link is not good. In the second one (named RIS-AE), the RIS is always employed at each hop. However, only the direct link or the relay link via the RIS is selected for the data transmission.
- Our proposed RIS-IC and RIS-AE methods reduce implementation complexity, as compared to the corresponding RIS-aided hop-by-hop transmission one proposed in [8] (named RIS-Opt).
- We derive expressions of the end-to-end block error rate (BLER-e2e) for the RIS-IC and RIS-AE over Rayleigh fading channels.
- All the derived BLER-e2e formulas will be validated by computer simulations.
- Impact of the important parameters such as the number of hops, the number of reflectors at the RIS, the threshold value in the RIS-IC scheme on the performance of the proposed schemes is investigated.

The remaining contents of this paper is outlined as follows: Section 2. presents system model of the RIS-IC and RIS-AE schemes. Derivation of the BLER-e2e performance over Rayleigh fading channel is performed in Section 3. . Simulation and theoretical results are presented in Section 4. , and Section 5. concludes the paper.

2. System Model

In Fig. 1, the source node (T_0) attempts to send the data to the destination node (T_N) via a pre-established N hop route, i.e., $\mathrm{T}_0 \to \mathrm{T}_1 \to ...\mathrm{T}_{N-1} \to \mathrm{T}_N$. The RIS ($R$) with K reflectors is deployed to assist the $\mathrm{T}_0 \to \mathrm{T}_N$ transmisison. We denote K elements of the RIS by R_k, $k = 1, 2, \ldots, K$. Assume that each node T_n $(n = 0, 1, ..., N)$ is equipped with single antenna, and therefore, the $\mathrm{T}_0 \to \mathrm{T}_N$ transmission is realized via N time slots. Using SPC, T_0 sends a δ-bit packet to T_N with a blocklength $m(m > 100)$, and the coding rate at each hop is given as $r = \delta/m$ [35].

Next, we denote $h_{\mathrm{T}_{n-1}\mathrm{T}_n}$, $h_{\mathrm{T}_{n-1}\mathrm{R}_k}$ and $h_{\mathrm{R}_k\mathrm{T}_n}$ as channel coefficients of the $\mathrm{T}_{n-1} \to \mathrm{T}_n$, $\mathrm{T}_{n-1} \to \mathrm{R}_k$ and $\mathrm{R}_k \to \mathrm{T}_n$ links, respectively, where $n = 1, ..., N$. Then, we denote the corresponding channel gains as $g_{\mathrm{T}_{n-1}\mathrm{T}_n} = |h_{\mathrm{T}_{n-1}\mathrm{T}_n}|^2$, $g_{\mathrm{T}_{n-1}\mathrm{R}_k} = |h_{\mathrm{T}_{n-1}\mathrm{R}_k}|^2$ and $g_{\mathrm{R}_k\mathrm{T}_n} = |h_{\mathrm{R}_k\mathrm{T}_n}|^2$. Once the $\mathrm{X} \to \mathrm{Y}$ channel is Rayleigh fading, g_{XY} has the following distribution functions:

$$\begin{aligned} f_{g_{\mathrm{XY}}}(x) &= \lambda_{\mathrm{XY}} \exp\left(-\lambda_{\mathrm{XY}} x\right), \\ F_{g_{\mathrm{XY}}}(x) &= 1 - \exp\left(-\lambda_{\mathrm{XY}} x\right), \end{aligned} \quad (1)$$

where $\mathrm{X} \in \{\mathrm{T}_{n-1}, \mathrm{R}_k\}$, $\mathrm{Y} \in \{\mathrm{T}_n, \mathrm{R}_k\}$. $f_{g_{\mathrm{XY}}}(.)$ and $F_{g_{\mathrm{XY}}}(.)$ denote probability density function (PDF) and cumulative distribution function (CDF) of g_{XY}, respectively, and $\lambda_{\mathrm{XY}} = d_{\mathrm{XY}}^{\beta}$ [36, 37] (β is a path-loss factor and d_{XY} is distance between X and Y).

For ease of presentation, we can denote the link distances as: $d_{\mathrm{T}_{n-1}\mathrm{R}_k} = d_{\mathrm{T}_{n-1}\mathrm{R}}$ and $d_{\mathrm{R}_k\mathrm{T}_n} = d_{\mathrm{RT}_n}$ for all R_k. Hence, we have $\lambda_{\mathrm{T}_{n-1}\mathrm{R}_k} = \lambda_{\mathrm{T}_{n-1}\mathrm{R}}$ and $\lambda_{\mathrm{R}_k\mathrm{T}_n} = \lambda_{\mathrm{RT}_n}$, for all R_k. Let P_{n-1} and σ_0^2 denote transmit power of T_{n-1} and variance of Gaussian

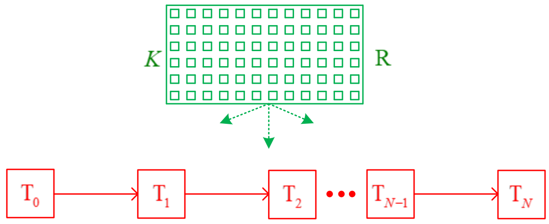

Fig. 1: System model of the proposed RISA-MHR-SPC model.

noises at all the receivers T_n, respectively. We also denote $\Delta_{n-1} = P_{\mathrm{T}_{n-1}}/\sigma_0^2$ as transmit signal-to-noise ratio (SNR).

Next, considering the hop in the RIS-IC scheme. If T_{n-1} directly the source packet to T_n, SNR of the $\mathrm{T}_{n-1} \to \mathrm{T}_n$ link is written as

$$\psi^{\mathrm{DT}}_{\mathrm{T}_{n-1}\mathrm{T}_n} = \frac{P_{\mathrm{T}_{n-1}} g_{\mathrm{T}_{n-1}\mathrm{T}_n}}{\sigma_0^2} = \Delta_{n-1} g_{\mathrm{T}_{n-1}\mathrm{T}_n}. \quad (2)$$

Using (1), the CDF of the SNR $\psi^{\mathrm{DT}}_{\mathrm{T}_{n-1}\mathrm{T}_n}$ can be obtained as

$$\begin{aligned} F_{\psi^{\mathrm{DT}}_{\mathrm{T}_{n-1}\mathrm{T}_n}}(x) &= \Pr\left(\psi^{\mathrm{DT}}_{\mathrm{T}_{n-1}\mathrm{T}_n} < x\right) \\ &= F_{g_{\mathrm{T}_{n-1}\mathrm{T}_n}}\left(\frac{x}{\Delta_{n-1}}\right) \\ &= 1 - \exp\left(-\frac{\lambda_{\mathrm{T}_{n-1}\mathrm{T}_n}}{\Delta_{n-1}} x\right). \end{aligned} \quad (3)$$

If $\psi^{\mathrm{DT}}_{\mathrm{T}_{n-1}\mathrm{T}_n}$ is higher than a pre-designed threshold (ψ_{th}), the direct link ($\mathrm{T}_{n-1} \to \mathrm{T}_n$) is used for the data transmission. Otherwise, if $\psi^{\mathrm{DT}}_{\mathrm{T}_{n-1}\mathrm{T}_n} \leqslant \psi_{\mathrm{th}}$, the RIS is employed, and the obtained maximal SNR of the $\mathrm{T}_{n-1} \to \mathrm{R} \to \mathrm{T}_n$ link can be given as in [25, Eq. (3)]:

$$\begin{aligned} \psi^{\mathrm{RIS}}_{\mathrm{T}_{n-1}\mathrm{T}_n} &= \frac{P_{\mathrm{T}_{n-1}}\left(\sum_{k=1}^{K} |h_{\mathrm{T}_{n-1}\mathrm{R}_k}||h_{\mathrm{R}_k\mathrm{T}_n}|\right)^2}{\sigma_0^2} \\ &= \Delta_{n-1}\left(Z_n^{\mathrm{sum}}\right)^2, \end{aligned} \quad (4)$$

where $Z_n^{\mathrm{sum}} = \sum_{k=1}^{K} |h_{\mathrm{T}_{n-1}\mathrm{R}_k}||h_{\mathrm{R}_k\mathrm{T}_n}|$ .Using [25, Eq. (13)], the CDF $F_{Z_n^{\mathrm{sum}}}(x)$ can be expressed as

$$F_{Z_n^{\mathrm{sum}}}(x) \approx \frac{\gamma(\alpha_n + 1, x/\omega_n)}{\Gamma(\alpha_n + 1)}, \quad (5)$$

where $\Gamma(.)$ and $\gamma(.)$ are Gamma function and lower incomplete Gamma function [38], respectively, and

$$\alpha_n = \frac{\left(\mathrm{E}\{Z_n^{\mathrm{sum}}\}\right)^2}{\mathrm{Var}\{Z_n^{\mathrm{sum}}\}} - 1,\ \omega_n = \frac{\mathrm{Var}\{Z_n^{\mathrm{sum}}\}}{\mathrm{E}\{Z_n^{\mathrm{sum}}\}}, \quad (6)$$

where, $\mathrm{E}\{Z_n^{\mathrm{sum}}\}$ and $\mathrm{Var}\{Z_n^{\mathrm{sum}}\}$ are expected value and variance of Z_n^{sum}, respectively. As [15, Eq. (13)], we have

$$\begin{aligned} \mathrm{E}\{Z_n^{\mathrm{sum}}\} &= \frac{K\pi}{4\sqrt{\lambda_{\mathrm{T}_{n-1}\mathrm{R}}\lambda_{\mathrm{RT}_n}}}, \\ \mathrm{Var}\{Z_n^{\mathrm{sum}}\} &= \frac{\left(16-\pi^2\right)K}{16\lambda_{\mathrm{T}_{n-1}\mathrm{R}}\lambda_{\mathrm{RT}_n}}. \end{aligned} \quad (7)$$

From (5), the CDF of the SNR $\psi^{\mathrm{RIS}}_{\mathrm{T}_{n-1}\mathrm{T}_n}$ in (4) is written as

$$\begin{aligned} F_{\psi^{\mathrm{RIS}}_{\mathrm{T}_{n-1}\mathrm{T}_n}}(x) &= F_{Z_n^{\mathrm{sum}}}\left(\sqrt{\frac{x}{\Delta_{n-1}}}\right) \\ &\approx \frac{1}{\Gamma(\alpha_n+1)}\gamma\left(\alpha_n+1, \frac{1}{\omega_n}\sqrt{\frac{x}{\Delta_{n-1}}}\right). \end{aligned} \quad (8)$$

Remark 1: When the $\mathrm{T}_{n-1} \to \mathrm{T}_n$ link is strong, T_{n-1} can sends the source bits directly to T_n without utilizing the RIS. Therefore, implementing the RIS-IC is simpler than that of the RIS-AE and the RIS-Opt. However, in the RIS-IC, the threshold ψ_{th} needs to be designed carefully. Indeed, if ψ_{th} is set to low values, the direct link is used more frequently than the relay link, and in this case, the RIS is not exploited effectively. Otherwise, if ψ_{th} is set to high values, the RIS is more frequently but the implementation complexity is higher.

Now, we consider the RISA-AE scheme; at the nth hop, the obtained SNR can be formulated as

$$\psi^{\mathrm{AE}}_{\mathrm{T}_{n-1}\mathrm{T}_n} = \max\left(\psi^{\mathrm{DT}}_{\mathrm{T}_{n-1}\mathrm{T}_n}, \psi^{\mathrm{RIS}}_{\mathrm{T}_{n-1}\mathrm{T}_n}\right). \quad (9)$$

where $\psi^{\mathrm{DT}}_{\mathrm{T}_{n-1}\mathrm{T}_n}$ and $\psi^{\mathrm{RIS}}_{\mathrm{T}_{n-1}\mathrm{T}_n}$ are given as in (2) and (4), respectively. Using (3) and (8), we can obtain the CDF of $\psi^{\mathrm{AE}}_{\mathrm{T}_{n-1}\mathrm{T}_n}$ as

$$\begin{aligned} F_{\psi^{\mathrm{AE}}_{\mathrm{T}_{n-1}\mathrm{T}_n}}(x) &= \Pr\left(\psi^{\mathrm{AE}}_{\mathrm{T}_{n-1}\mathrm{T}_n} < x\right) \\ &= F_{\psi^{\mathrm{DT}}_{\mathrm{T}_{n-1}\mathrm{T}_n}}(x) F_{\psi^{\mathrm{RIS}}_{\mathrm{T}_{n-1}\mathrm{T}_n}}(x) \\ &= \left(1 - \exp\left(-\frac{\lambda_{\mathrm{T}_{n-1}\mathrm{T}_n}}{\Delta_{n-1}}x\right)\right) \\ &\times \frac{1}{\Gamma(\alpha_n+1)}\gamma\left(\alpha_n+1, \frac{1}{\omega_n}\sqrt{\frac{x}{\Delta_{n-1}}}\right). \end{aligned} \quad (10)$$

Remark 2: Equation (9) implies that the direct link ($\mathrm{T}_{n-1} \to \mathrm{T}_n$) is chosen if $\psi^{\mathrm{DT}}_{\mathrm{T}_{n-1}\mathrm{T}_n} \geqslant \psi^{\mathrm{RIS}}_{\mathrm{T}_{n-1}\mathrm{T}_n}$. Otherwise, the relay link is selected. This also means that when the direct link is better than the relay link (e.g., the RIS is far T_{n-1} and T_n or T_{n-1} and T_n are close each other), the direct link is used. Hence, the RIS-AE achieves better performance, but the implementation of the RIS-AE is more complex than that of the RIS-IC.

For performance comparison, this paper also introduces the RIS-Opt scheme. In this scheme, the SNR at the nth hop determined by an optimal phase shift strategy, and it is provided similarly to [18, Eq. (3)], as

$$\psi^{\mathrm{Opt}}_{\mathrm{T}_{n-1}\mathrm{T}_n} = \Delta_{\mathrm{T}_{n-1}}\left(|h_{\mathrm{T}_{n-1}\mathrm{T}_n}| + \sum_{k=1}^{K}|h_{\mathrm{T}_{n-1}\mathrm{R}_k}||h_{\mathrm{R}_k\mathrm{T}_n}|\right)^2 \quad (11)$$

Note that $\psi^{\mathrm{Opt}}_{\mathrm{T}_{n-1}\mathrm{T}_n} \geqslant \psi^{\mathrm{AE}}_{\mathrm{T}_{n-1}\mathrm{T}_n}$ $(\forall n)$, which means the RIS-Opt outperforms the RIS-AE. However, implementing the RIS-Opt is most complex due to the optimal phase shift strategy [18].

Next, we analyze BLER-e2e of the Z scheme, where $Z \in \{\mathrm{RIS\text{ - }IC}, \mathrm{RIS\text{ - }AE}\}$. When the selective decode-and-forward technique is applied, BLER-e2e of the Z scheme can be expressed as in [35] as

$$\mathrm{BLER}^{\mathrm{Z}}_{\mathrm{e2e}} = \mathrm{BLER}^{\mathrm{Z}}_{1} + \sum_{n=2}^{N}\left[\mathrm{BLER}^{\mathrm{Z}}_{n} \times \prod_{u=1}^{n-1}\left(1-\mathrm{BLER}^{\mathrm{Z}}_{u}\right)\right], \quad (12)$$

where $\mathrm{BLER}^{\mathrm{Z}}_{n}$ is BLER at the nth hop in the Z scheme, $\left(1-\mathrm{BLER}^{\mathrm{Z}}_{u}\right)$ denotes the successful decoding at the u-th hop, and $\mathrm{BLER}^{\mathrm{Z}}_{n} \times \prod_{u=1}^{n-1}\left(1-\mathrm{BLER}^{\mathrm{Z}}_{u}\right)$ implies that the source packet is dropped at the nth hop.

3. Performance Analysis

In this section, we derive expressions of $\mathrm{BLER}^{\mathrm{Z}}_{n}$, and then substituting the derived $\mathrm{BLER}^{\mathrm{Z}}_{n}$ into (12) to obtain $\mathrm{BLER}^{\mathrm{Z}}_{\mathrm{e2e}}$ of the Z scheme.

At first, we considering the RIS-IC scheme; BLER at nth hop in this scheme can be formulated as

$$\mathrm{BLER}^{\mathrm{RIS\text{ - }IC}}_{n} = \mathrm{BLER}^{\mathrm{RIS\text{ - }IC}}_{n,\mathrm{DT}} + \Pr\left(\psi^{\mathrm{DT}}_{\mathrm{T}_{n-1}\mathrm{T}_n} \leqslant \psi_{\mathrm{th}}\right)\mathrm{BLER}^{\mathrm{RIS\text{ - }IC}}_{n,\mathrm{RIS}}. \quad (13)$$

In (13), $\mathrm{BLER}^{\mathrm{RIS\text{ - }IC}}_{n,\mathrm{DT}}$ and $\mathrm{BLER}^{\mathrm{RIS\text{ - }IC}}_{n,\mathrm{RIS}}$ are BLERs in the cases where the direct and relay links are used, respectively. Also in (13), $\Pr\left(\psi^{\mathrm{DT}}_{\mathrm{T}_{n-1}\mathrm{T}_n} \leqslant \psi_{\mathrm{th}}\right)$ is probability that the RIS is used, and it is calculated as

$$\Pr\left(\psi^{\mathrm{DT}}_{\mathrm{T}_{n-1}\mathrm{T}_n} \leqslant \psi_{\mathrm{th}}\right) = F_{\psi^{\mathrm{DT}}_{\mathrm{T}_{n-1}\mathrm{T}_n}}(\psi_{\mathrm{th}}) = 1-\exp\left(-\frac{\lambda_{\mathrm{T}_{n-1}\mathrm{T}_n}}{\Delta_{n-1}}x\right). \quad (14)$$

For $\mathrm{BLER}^{\mathrm{RIS\text{ - }IC}}_{n,\mathrm{DT}}$ in (13), we can formulate it as (see [35]):

$$\mathrm{BLER}^{\mathrm{RIS\text{ - }IC}}_{n,\mathrm{DT}} \approx \int_0^{+\infty} Q\left(\frac{C(x)-r}{\sqrt{V(x)/m}}\right) \times f_{\psi^{\mathrm{DT}}_{\mathrm{T}_{n-1}\mathrm{T}_n}|\psi^{\mathrm{DT}}_{\mathrm{T}_{n-1}\mathrm{T}_n}>\psi_{\mathrm{th}}}(x)\,dx, \quad (15)$$

where $Q(.)$ is Gaussian Q-function [38], $V(x)$ and $C(x)$ are given, respectively as (see [35]):

$$V(x) = \left(1-\frac{1}{(1+x)^2}\right)(\log_2(e))^2, \quad C(x) = \log_2(1+x). \quad (16)$$

In (15), $f_{\psi^{\mathrm{DT}}_{\mathrm{T}_{n-1}\mathrm{T}_n}|\psi^{\mathrm{DT}}_{\mathrm{T}_{n-1}\mathrm{T}_n}>\psi_{\mathrm{th}}}(x)$ is the PDF of $\psi^{\mathrm{DT}}_{\mathrm{T}_{n-1}\mathrm{T}_n}$ conditioned on $\psi^{\mathrm{DT}}_{\mathrm{T}_{n-1}\mathrm{T}_n} > \psi_{\mathrm{th}}$. To find $f_{\psi^{\mathrm{DT}}_{\mathrm{T}_{n-1}\mathrm{T}_n}|\psi^{\mathrm{DT}}_{\mathrm{T}_{n-1}\mathrm{T}_n}>\psi_{\mathrm{th}}}(x)$, we first find the conditioned CDF $F_{\psi^{\mathrm{DT}}_{\mathrm{T}_{n-1}\mathrm{T}_n}|\psi^{\mathrm{DT}}_{\mathrm{T}_{n-1}\mathrm{T}_n}>\psi_{\mathrm{th}}}(x)$:

$$\begin{aligned} &F_{\psi^{\mathrm{DT}}_{\mathrm{T}_{n-1}\mathrm{T}_n}|\psi^{\mathrm{DT}}_{\mathrm{T}_{n-1}\mathrm{T}_n}>\psi_{\mathrm{th}}}(x) \\ &= \Pr\left(\psi^{\mathrm{DT}}_{\mathrm{T}_{n-1}\mathrm{T}_n} < x, \psi^{\mathrm{DT}}_{\mathrm{T}_{n-1}\mathrm{T}_n} > \psi_{\mathrm{th}}\right) \\ &= \begin{cases} 0, & x \leqslant \psi_{\mathrm{th}} \\ \exp\left(-\dfrac{\lambda_{\mathrm{T}_{n-1}\mathrm{T}_n}\psi_{\mathrm{th}}}{\Delta_{n-1}}\right) - \exp\left(-\dfrac{\lambda_{\mathrm{T}_{n-1}\mathrm{T}_n}x}{\Delta_{n-1}}\right), & x > \psi_{\mathrm{th}} \end{cases} \end{aligned} \quad (17)$$

From (17), we obtain the conditioned PDF $f_{\psi^{\mathrm{DT}}_{\mathrm{T}_{n-1}\mathrm{T}_n}|\psi^{\mathrm{DT}}_{\mathrm{T}_{n-1}\mathrm{T}_n}>\psi_{\mathrm{th}}}(x)$ as

$$f_{\psi_{\mathrm{T}_{n-1}\mathrm{T}_n}|\psi_{\mathrm{T}_{n-1}\mathrm{T}_n}>\psi_{\mathrm{th}}}(x) = \begin{cases} 0, & x \leqslant \psi_{\mathrm{th}} \\ \dfrac{\lambda_{\mathrm{T}_{n-1}\mathrm{T}_n}x}{\Delta_{n-1}}\exp\left(-\dfrac{\lambda_{\mathrm{T}_{n-1}\mathrm{T}_n}x}{\Delta_{n-1}}\right), & x > \psi_{\mathrm{th}} \end{cases} \quad (18)$$

Substituting (18) into (15), we have

$$\mathrm{BLER}^{\mathrm{RIS\text{ - }IC}}_{n,\mathrm{DT}} \approx \int_{\psi_{\mathrm{th}}}^{+\infty} Q\left(\frac{C(x)-r}{\sqrt{V(x)/m}}\right) \times \frac{\lambda_{\mathrm{T}_{n-1}\mathrm{T}_n}x}{\Delta_{n-1}}\exp\left(-\frac{\lambda_{\mathrm{T}_{n-1}\mathrm{T}_n}x}{\Delta_{n-1}}\right)dx. \quad (19)$$

Similarly, $\mathrm{BLER}^{\mathrm{RIS\text{ - }IC}}_{n,\mathrm{RIS}}$ in (13) can be expressed as

$$\mathrm{BLER}^{\mathrm{RIS\text{ - }IC}}_{n,\mathrm{RIS}} \approx \int_0^{+\infty} Q\left(\frac{C(x)-r}{\sqrt{V(x)/m}}\right) f_{\psi^{\mathrm{RIS}}_{\mathrm{T}_{n-1}\mathrm{T}_n}}(x)\,dx. \quad (20)$$

Moreover, $\mathrm{BLER}^{\mathrm{RIS\text{ - }IC}}_{n,\mathrm{RIS}}$ in (20) can be rewritten under the following form (see [35, Eq. (11)]):

$$\mathrm{BLER}^{\mathrm{RIS\text{ - }IC}}_{n,\mathrm{RIS}} \approx \vartheta\sqrt{m}\int_{\rho_L}^{\rho_H} F_{\psi^{\mathrm{RIS}}_{\mathrm{T}_{n-1}\mathrm{T}_n}}(x)dx, \quad (21)$$

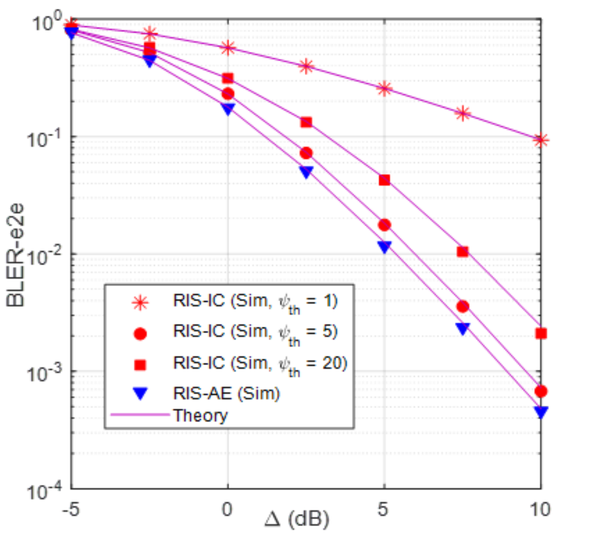

Fig. 2: BLER-e2e as a function of Δ(dB) when $N = 2$ and $K = 3$.

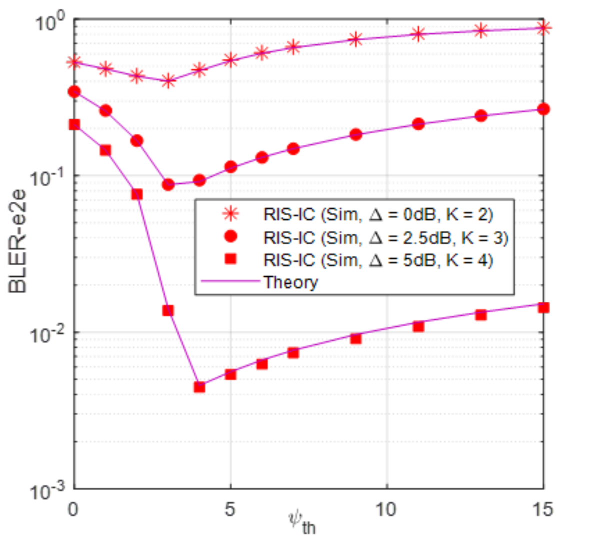

Fig. 3: BLER-e2e as a function of ψ_{th} when $N = 4$.

where

$$\vartheta = \frac{1}{2\pi\sqrt{2^{2r}-1}}, \theta = 2^r - 1,$$
$$\rho_H = \theta + \frac{1}{2\vartheta\sqrt{m}}, \rho_L = \theta - \frac{1}{2\vartheta\sqrt{m}}. \quad (22)$$

Substituting (8) into (21), after some careful manipulation, we obtain

$$\begin{aligned}\text{BLER}_{n,\text{RIS}}^{\text{RIS - IC}} &\approx \frac{\vartheta\sqrt{m}}{\Gamma(\alpha_n+1)} \\ &\times \int_{\rho_L}^{\rho_H} \gamma\left(\alpha_n+1, \frac{1}{\omega_n}\sqrt{\frac{x}{\Delta_{n-1}}}\right)dx \\ &\approx \frac{\vartheta\sqrt{m}}{\Gamma(\alpha_n+1)}\left(I_{n,\text{H}} - I_{n,\text{L}}\right), \end{aligned} \quad (23)$$

where

$$\begin{aligned} I_{n,\text{H}} &= \rho_H \gamma\left(1+\alpha_n, \frac{\sqrt{\rho_H}}{\omega_n\sqrt{\Delta_{n-1}}}\right) \\ &- \frac{1}{(\omega_n)^2\Delta_{n-1}}\gamma\left(3+\alpha_n, \frac{\sqrt{\rho_H}}{\omega_n\sqrt{\Delta_{n-1}}}\right), \\ I_{n,\text{L}} &= \rho_L \gamma\left(1+\alpha_n, \frac{\sqrt{\rho_L}}{\omega_n\sqrt{\Delta_{n-1}}}\right) \\ &- \frac{1}{(\omega_n)^2\Delta_{n-1}}\gamma\left(3+\alpha_n, \frac{\sqrt{\rho_L}}{\omega_n\sqrt{\Delta_{n-1}}}\right), \end{aligned} \quad (24)$$

Substituting (14), (19) and (23) into (13), we can obtain $\text{BLER}_n^{\text{RIS - IC}}$ as follows:

$$\begin{aligned}\text{BLER}_n^{\text{RIS - IC}} &\approx \int_{\psi_{\text{th}}}^{+\infty} Q\left(\frac{C(x)-r}{\sqrt{V(x)/m}}\right) \\ &\times \frac{\lambda_{\text{T}_{n-1}\text{T}_n}x}{\Delta_{n-1}} \exp\left(-\frac{\lambda_{\text{T}_{n-1}\text{T}_n}x}{\Delta_{n-1}}\right)dx \\ &+ \left(1-\exp\left(-\frac{\lambda_{\text{T}_{n-1}\text{T}_n}}{\Delta_{n-1}}x\right)\right) \\ &\times \frac{\vartheta\sqrt{m}}{\Gamma(\alpha_n+1)}\left(I_{n,\text{H}} - I_{n,\text{L}}\right). \end{aligned} \quad (25)$$

Similar to (21), we can calculate $\text{BLER}_n^{\text{RIS - AE}}$ as

$$\text{BLER}_n^{\text{RIS - AE}} \approx \vartheta\sqrt{m}\int_{\rho_L}^{\rho_H} F_{\psi^{\text{RIS}}_{\text{T}_{n-1}\text{T}_n}}(x)dx. \quad (26)$$

Substituting (10) into (26), we have

$$\begin{aligned}\text{BLER}_n^{\text{RIS - AE}} &\approx \frac{\vartheta\sqrt{m}}{\Gamma(\alpha_n+1)} \\ &\times \int_{\rho_L}^{\rho_H}\left[\left(1-\exp\left(-\frac{\lambda_{\text{T}_{n-1}\text{T}_n}}{\Delta_{n-1}}x\right)\right)\right. \\ &\left.\times\, \gamma\left(\alpha_n+1, \frac{1}{\omega_n}\sqrt{\frac{x}{\Delta_{n-1}}}\right)\right]dx. \end{aligned} \quad (27)$$

Finally, substituting (25) and (27) into (12), we obtain expressions of $\text{BLER}_{\text{e2e}}^{\text{RIS - IC}}$ and $\text{BLER}_{\text{e2e}}^{\text{RIS - AE}}$, respectively.

4. Results

This section provides both simulation results (Monte Carlo simulation) and theoretical results of the BLER-

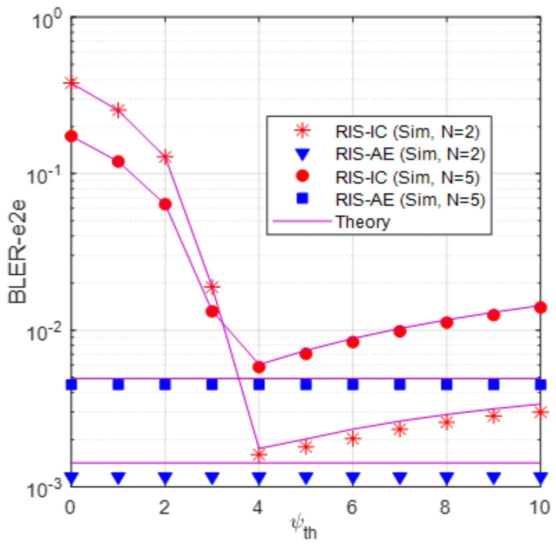

Fig. 4: BLER-e2e as a function of ψ_{th} when $K = 4$ and $\Delta =$ 5dB.

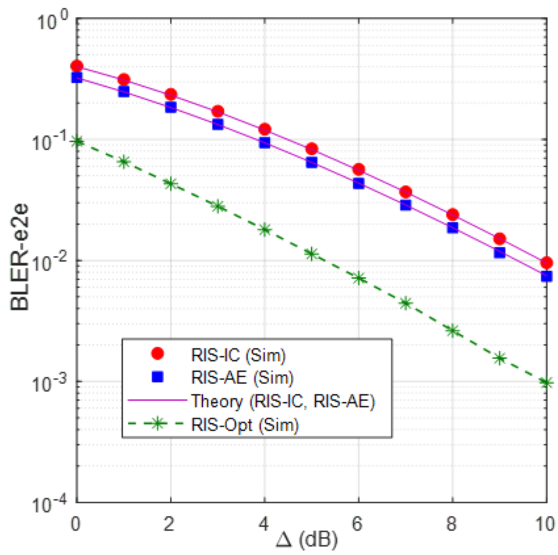

Fig. 5: BLER-e2e as a function of Δ(dB) when $K = 2$, $N = 6$ and $\psi_{\text{th}} = 4$.

e2e performance of the RIS-IC and RIS-AE schemes. For a fair comparison, the total transmit power is fixed by P_{tot}, i.e., $\sum_{n=0}^{N-1} P_{\text{T}_n} = P_{\text{tot}}$. We also assume that all the transmitters have the same transmit power, and we hence have $P_{\text{T}_n} = P_{\text{tot}}/N$. In all simulations, we place T_n at position $(n/N, 0)$ and the RIS at $(0.5, 0.75)$. We also fix the values of the parameters as follows: $\beta = 3$, $\sigma_0^2 = 1$, $\delta = 256$ and $m = 128$.

Fig. 2 depicts the BLER-e2e performance of the RIS-IC and RIS-AE schemes as a function of transmit SNR $\left(\Delta = P_{\text{tot}}/\sigma_0^2\right)$ in dB with different values of the threshold ψ_{th}, i.e., $\psi_{\text{th}} \in \{1, 5, 20\}$. The remaining parameters are set to $N = 2$ and $K = 3$. As observed, BLER-e2e of the RIS-AE is consistently lower than that of the RIS-IC for all values of ψ_{th}. It is evident that the threshold ψ_{th} significantly impacts the performance of the RIS-IC. Specifically, when $\psi_{\text{th}} = 1$, BLER-e2e of the RIS-IC is highest, whereas with $\psi_{\text{th}} = 5$, it reaches to the lowest value. As highlighted in Remark 1, a very low value of ψ_{th} implies that the RIS-IC predominantly utilizes the direct link for data transmission at each hop. Conversely, with a very high value of ψ_{th}, the relay link is predominantly used, resulting in the omission of the role of the direct link. This explains why BLER-e2e of the RIS-IC with $\psi_{\text{th}} = 20$ is higher than that with $\psi_{\text{th}} = 5$. Finally, Fig. 2 illustrates that the simulation (Sim) and theoretical (Theory) results are in a good agreement, confirming the correctness of our derivations in the previous sections.

Fig. 3 illustrates the BLER-e2e performance of the RIS-IC as a function of ψ_{th} with $N = 4$ and varying values of Δ and K. As expected, BLER-e2e of the RIS-IC is lower with higher values of Δ and K. Furthermore, Fig. 3 reveals presence of an optimal value for ψ_{th} that minimizes BLER-e2e of the RIS-IC. For instance, in Fig. 3, with $\Delta = 0$dB, $K = 2$ and $\Delta = 2.5$dB, $K = 3$, the optimal value of ψ_{th} is 3. Similarly, with $\Delta = 5$dB, $K = 5$, the optimal value of ψ_{th} is 4. This highlights the need for careful design considerations when selecting ψ_{th} to optimize the performance of the RIS-IC.

Fig. 4 illustrates BLER-e2e of the RIS-IC and RIS-AE schemes as a function of ψ_{th} with $K = 4$ and $\Delta = 5$dB. In this figure, the number of hops (N) is set to 2 and 5. Similar to Fig. 3, it is evident that an optimal value of ψ_{th} exists so that the performance of the RIS-IC is best. For instance, the optimal value of ψ_{th} is 4 in both cases of $N = 2$ and $N = 5$. However, it is worth noting that the RIS-AE consistently outperforms the RIS-IC for all values of ψ_{th}. To find the optimal values of ψ_{th}, the derived expressions of BLER can be used efficiently. Additionally, we observe that the number of hops significantly influences the BLER-e2e performance. In the RIS-AE scheme, the BLER-e2e value is lower with $M = 2$, and in the RIS-IC scheme, the performance is superior with $N = 2$ and $\psi_{\text{th}} \geqslant 4$.

Fig. 5 compares the performacne of the RIS-IC, RIS-AE and RIS-Opt schemes with $K = 2$, $N = 6$ and $\psi_{\text{th}} = 4$. As observed, the RIS-Opt achieves the best performance, while the RIS-AE again outperforms the RIS-IC. As mentioned earlier, implementing the RIS-Opt is the most complex because it requires all channel state information of the links for realizing the optimal phase shift strategy. Additionally, it is worth noting that the performance gap between the RIS-AE and the

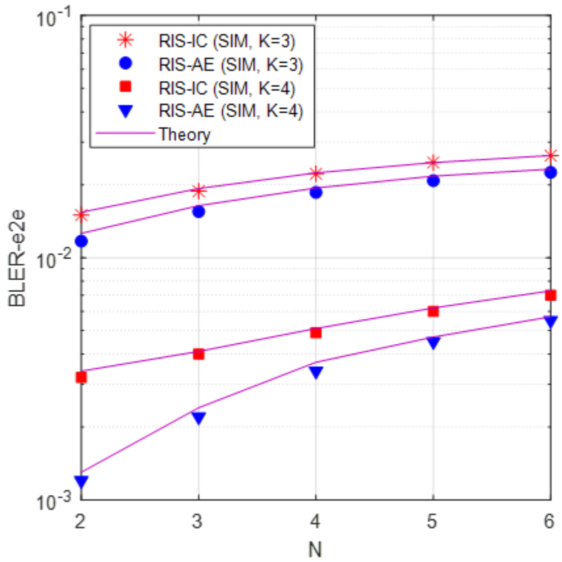

Fig. 6: BLER-e2e as a function of N when $\psi_{\text{th}} = 3.5$ and $\Delta = 5$(dB).

RIS-IC is small because ψ_{th} is designed with an appropriate value, i.e., $\psi_{\text{th}} = 4$.

Fig. 6 presents the performance of the RIS-IC and RIS-AE schemes as a function of the number of hops (N) when $\psi_{\text{th}} = 3.5$ and $\Delta = 5$(dB). Fig. 6 demonstrates that BLER-e2e of the RIS-IC and RIS-AE schemes increases with the increasing of N. It is due to the fact that when the number of hops increases, the transmit power of each node decreases due to the fixed total transmit power, i.e., $P_{\text{T}_n} = P_{\text{tot}}/N$ for all $n = 0, 1, ..., N-1$. Again, we can see that the performance of the proposed schemes is better with higher number of reflectors at the RIS.

5. Conclusion

In this paper, we proposed two RIS-aided multi-hop relaying schemes using SPC. Implementing the proposed RIS-IC and RIS-AE schemes are much simpler than the RIS-Opt one. We evaluated the BLER-e2e performance of the proposed schemes through both simulations and analysis. The results indicated that the RIS-AE outperforms the RIS-IC although the implementation of the RIS-IC is simpler. In the RIS-IC, the threshold needs to be optimized to achieve the best performance. Furthermore, the BLER-e2e performance of the proposed schemes can be enhanced by increasing the transmit power and the number of reflectors at the RIS.

Acknowledgment

This research is funded by Posts and Telecommunications Institute of Technology under grant number 11-2023-HV-VT2.

Author Contributions

The main contributions of Pham Minh Quang and Ngo Hoang An were to create the main ideas and execute performance evaluation by extensive simulations, while Tran Trung Duy, Nguyen Tien Tung and Anh-Vu Le worked as the advisers of Pham Minh Quang and Ngo Hoang An to discuss, create, and advise the main ideas and performance evaluations together.

References

[1] TIN, P. T., HUNG, D. T., DUY, T. T. and VOZNAK, M. Security-Reliability Analysis of NOMA – Based Multi-Hop Relay Networks In Presence Of an Active Eavesdropper With Imperfect Eavesdropping CSI. *Advances in Electrical and Electronic Engineering*. 2017, vol. 15, iss. 04, pp. 591-597. ISSN 1336-1376. DOI: 10.15598/aeee.v15i4.2386.

[2] DUC, N. V., LUAN, N. T., TIN, P. T. and VINH, N. V. Reliability-Security in Wireless-Powered Cooperative Network with Friendly Jammer. *Advances in Electrical and Electronic Engineering*. 2023, vol. 20, iss. 04, pp. 584-591. ISSN 1336-1376. DOI: 10.15598/aeee.v20i4.4511.

[3] LUAN, N. T., LONG, N. T., VINH, N. V. and TIN, P. T. Outage Performance of Full-Duplex Unmanned Aerial Vehicle-aided Cooperative Non-orthogonal Multiple Access. *Advances in Electrical and Electronic Engineering*. 2023, vol. 21, iss. 03, pp. 1-8. ISSN 1336-1376. DOI: 10.15598/aeee.v21i1.4515.

[4] HIEU, T. D., DUY T. T. and KIM, B. S. Performance Enhancement for Multi-hop Harvest-to-Transmit WSNs With Path-Selection Methods in Presence of Eavesdroppers and Hardware Noises. *IEEE Sensors Journal*. 2018, vol. 18, iss. 12, pp. 5173 – 5186. ISSN 1530-437X. DOI: 10.1109/JSEN.2018.2829145.

[5] TU, T. L., et al. Performance Analysis of Multi-hop Full-duplex NOMA Systems With Imperfect Interference Cancellation and Near-Field Path-Loss. *Sensors*. 2023, vol. 23, iss. 01, ID 524. ISSN 1424-8220. DOI: 10.3390/s23010524.

[6] TAN, N. N., et al. On the Dilemma of Reliability or Security in Unmanned Aerial Vehicle Communications Assisted by Energy Harvesting Relaying. *IEEE Journal on Selected Areas in Communications*. 2024, vol. 42, iss. 01, pp. 52-67. ISSN 0733-8716. DOI: 10.1109/JSAC.2023.3322756.

[7] TAN, N. N., et al. Security-Reliability Tradeoffs for Satellite–Terrestrial Relay Networks With a Friendly Jammer and Imperfect CSI. *IEEE Transactions on Aerospace and Electronic Systems*. 2023, vol. 59, iss. 05, pp. 7004-7019. ISSN: 0018-9251. DOI: 10.1109/TAES.2023.3282934.

[8] TAN, N. N., et al. Physical Layer Security in AF-Based Cooperative SWIPT Sensor Networks. *IEEE Sensors Journal*. 2023, vol. 23, iss. 1, pp. 689-705. ISSN 1530-437X. DOI: 10.1109/JSEN.2022.3224128.

[9] TU, T. L., et al. Broadcasting in Cognitive Radio Networks: A Fountain Codes Approach. *IEEE Transactions on Vehicular Technology*. 2022, vol. 71, iss. 10, pp. 11289-11294. ISSN 0018-9545. DOI: 10.1109/TVT.2022.3188969.

[10] TAN, N. N., et al. Outage Performance of Satellite Terrestrial Full-Duplex Relaying Networks With co-Channel Interference. *IEEE Wireless Communications Letters*. 2022, vol. 11, iss. 7, pp. 1478-1482. ISSN 2162-2337. Doi: 10.1109/LWC.2022.3175734.

[11] TAN, N. N., et al. Partial and Full Relay Selection Algorithms for AF Multi-Relay Full-Duplex Networks With Self-Energy Recycling in Non-Identically Distributed Fading Channels. *IEEE Transactions on Vehicular Technology*. 2022, vol. 71, iss. 6, pp. 6173-6188. ISSN 0018-9545. DOI: 10.1109/TVT.2022.3158340.

[12] PHU, L. S., et al. Improving the Capacity of NOMA Network Using Multiple Aerial Intelligent Reflecting Surfaces. *IEEE Access*. 2023, vol. 11, pp. 107958-107971. ISSN: 2169-3536. DOI: 10.1109/ACCESS.2023.3319675.

[13] NGUYEN, H., et al. Security-Reliability Analysis in CR-NOMA IoT Network Under I/Q Imbalance. *IEEE Access*. 2023. vol. 11, pp. 119045-119056. ISSN 2169-3536. DOI: 10.1109/ACCESS.2023.3327789.

[14] LE, A. T., et al. Performance Analysis of RIS-Assisted Ambient Backscatter Communication Systems. *IEEE Wireless Communications Letters*. 2024, vol. 13, iss. 3, pp. 791-795. ISSN 2162-2337. DOI: 10.1109/LWC.2023.3344113.

[15] TAN, N. N., et al. On performance of RIS-aided bidirectional full-duplex systems with combining of imperfect conditions. *Wireless Networks*. 2024, vol. 30, pp. 649–660. ISSN 1022-0038. DOI: 10.1007/s11276-023-03490-7.

[16] WU, Q., et al. Intelligent Reflecting Surface-Aided Wireless Communications: A Tutorial. *IEEE Transactions on Communications*. 2021, vol. 69, iss. 05, pp. 3313-3351. ISSN 0090-6778. DOI: 10.1109/TCOMM.2021.3051897.

[17] GONG, S., et al. Toward Smart Wireless Communications via Intelligent Reflecting Surfaces: A Contemporary Survey. *IEEE Communications Surveys & Tutorials*. 2020, vol. 22, iss. 04, pp. 2283-2314. ISSN 1553877X. DOI: 10.1109/COMST.2020.3004197.

[18] CHIEN, T. V., TU, T. L., CHATZINOTAS, S. and OTTERSTEN, B. Coverage Probability and Ergodic Capacity of Intelligent Reflecting Surface-Enhanced Communication Systems. *IEEE Communications Letters*. 2021, vol. 25, iss. 01, pp. 69-73. ISSN 1089-7798. DOI: 10.1109/LCOMM.2020.3023759.

[19] YANG, L., et al. Secrecy Performance Analysis of RIS-Aided Wireless Communication Systems. *IEEE Transactions on Vehicular Technology*. 2020, vol. 69, iss. 10, pp. 12296-12300. ISSN 0018-9545. DOI: 10.1109/TVT.2020.3007521.

[20] XU, P., CHEN, G., PAN G. and RENZO, M. D. Ergodic Secrecy Rate of RIS-Assisted Communication Systems in the Presence of Discrete Phase Shifts and Multiple Eavesdroppers. *IEEE Wireless Communications Letters*. 2021, vol. 10, iss. 3, pp. 629-633. ISSN 2162-2345. DOI: 10.1109/LWC.2020.3044178.

[21] AI, Y., et al. Secure Vehicular Communications Through Reconfigurable Intelligent Surfaces. *IEEE Transactions on Vehicular Technology*. 2021, vol. 70, iss. 7, pp. 7272-7276. ISSN 0018-9545. DOI: 10.1109/TVT.2021.3088441.

[22] LINH, N. T. Y., TU, N. H., SON, P. N., BAO, V. N. Q. Dual-hop relaying networks for short-packet URLLCs: Performance analysis and optimization. *Journal of Communications and Networks*. 2022, vol. 24, iss. 04, pp. 408-418. ISSN 1229-2370. DOI: 10.23919/JCN.2022.000020.

[23] VAN, N. T., DINH, N. V., COSTA, D. B. da, AN, B. Short-Packet Communications in Multi-Hop WPINs: Performance Analysis and Deep Learning Design. In: *2021 IEEE Global Communications Conference (GLOBECOM)*. Madrid, Spain, 2021, pp. 1–6. ISBN 978-1-7281-8104-2.

[24] VAN, N. T., et al. Short-Packet Communications in Multi Hop Networks with WET: Performance Analysis and Deep Learning-Aided Optimization. *IEEE Transactions on Wireless Communications*. 2023, vol. 22, iss. 1, pp. 439-456. ISSN 1536-1276. DOI: 10.1109/TWC.2022.3195234.

[25] SON, P. N., DUY, T. T., TUAN, P. V. and PHUOC, H. V. Short packet communication in Underlay Cognitive Network assisted by Intelligent Reflecting Surface. *ETRI Journal*. 2023, vol. 45, iss. 1, pp. 28-44. ISSN 1225-6463. DOI: 10.4218/etrij.2021-0435.

[26] HUAN, N. T., et al. Incremental Cooperation Based Multi-hop Relaying Scheme With Fountain Codes, Wirelessly Energy Harvesting and Partial Relay Selection. In: *2022 International Conference on Advanced Technologies for Communications (ATC)*. HaNoi, Vietnam, 2022, pp. 338-343. ISBN 978-1-6654-5188-8.

[27] AN, N. H., et al. Performance Evaluation Of Multi-Hop Relaying IoTs Networks Using Hop-By-Hop Cooperative Transmission Under Impact of Co-channel Interference. In: *The Seventh International Conference on Research in Intelligent Computing in Engineering (RICE 2022)*. HungYen, Vietnam, 2022, pp. 63-68. ISBN 978-83-965897-6-7.

[28] HASHEMI, R., ALI, S., MAHMOOD, N. H. and LATVA-AHO, M. Average Rate and Error Probability Analysis in Short Packet Communications Over RIS-Aided URLLC Systems. *IEEE Transactions on Vehicular Technology*. 2021, vol. 70, iss. 10, pp. 10320-10334. ISSN 0018-9545. DOI: 10.1109/TVT.2021.3105878.

[29] ZHANG, K., WANG, K., YANG, K. and ZHANG, G. IRS-Assisted Short Packet Wireless Energy Transfer and Communications. *IEEE Wireless Communications Letters*. 2022, vol. 11, iss. 2, pp. 303-307. ISSN 2162-2345. DOI: 10.1109/LWC.2021.3126596.

[30] VU, T. H., VAN, N. T., COSTA, D. B. d. and KIM, S. Intelligent Reflecting Surface-Aided Short-Packet Non-Orthogonal Multiple Access Systems. *IEEE Transactions on Vehicular Technology*. 2022, vol. 71, iss. 4, pp. 4500-4505. ISSN 0018-9545. DOI: 10.1109/TVT.2022.3146856.

[31] VU, T. H., VAN, N. T., VIET, P. Q., COSTA D. B. da. and KIM, S. STAR-RIS-Enabled Short-Packet NOMA Systems. *IEEE Transactions on Vehicular Technology*. 2023, vol. 72, iss. 10, pp. 13764-13769. ISSN 0018-9545. DOI: 10.1109/TVT.2023.3278737.

[32] YUAN, L., DU, Q., YANG, F. and YANG, N. Performance Analysis of IRS-Aided Short-Packet NOMA Systems Over Nakagami-m Fading Channels. *IEEE Transactions on Vehicular Technology*. 2023, vol. 72, iss. 6, pp. 8228-8233. ISSN 0018-9545. DOI: 10.1109/TVT.2023.3243998.

[33] SHARMA, P. K., SHARMA, N., DHOK, S. and SINGH, A. RIS-Assisted FD Short Packet Communication With Non-Linear EH. *IEEE Communications Letters*. 2023, vol. 27, iss. 2, pp. 522-526. ISSN 1089-7798. DOI: 10.1109/LCOMM.2022.3223286.

[34] TY, V. T., et al. Security-Reliability Tradeoff of Multi-hop Secure Communication Networks Using Fountain Codes and RIS-aided Cooperative Communication. In: *2023 International Conference on Advanced Technologies for Communications (ATC)*. Da Nang, Vietnam, 2023, pp. 499-504. ISBN 979-8-3503-0132-8.

[35] TU, N. H. and LEE, K. Performance Analysis and Optimization of Multihop MIMO Relay Networks in Short-Packet Communications. *IEEE Transactions on Wireless Communications*. 2022, vol. 21, iss. 6, pp. 4549-4562. DOI: 10.1109/TWC.2021.3131205.

[36] TIN, P. T., HUNG, D. T., DUY, T. T. and VOZNAK, M. Phu Tran Tin, Dang The Hung, Tran Trung Duy, M. Analysis of Probability of Non-zero Secrecy Capacity for Multi-hop Networks in Presence of Hardware Impairments over Nakagami-m Fading Channels. *Radioengineering*. 2016, vol. 25, iss. 04, pp. 774-782. ISSN 1210-2512. DOI: 10.13164/re.2016.0774.

[37] HA, D. H., et al. Security-Reliability Trade-Off Analysis for Rateless Codes-Based Relaying Protocols Using NOMA, Cooperative Jamming and Partial Relay Selection. *IEEE Access*. 2021, vol. 9, pp. 131087-131108. ISSN 2169-3536. DOI: 10.1109/ACCESS.2021.3114343.

[38] GRADSHTEYN, I. S. and RYZHIK I. M. *Table of Integrals, Series, and Products*. Boston: Academic Press, 2007. ISBN 978-0-12-384933-5.

About Authors

Pham Minh QUANG received Bachelor and Master degrees from University of Science, National University of Ho Chi Minh City in 2007 and 2012, respectively. Currently, he is working at Department of Telecommunications 2, Posts and Telecommunications Institute of Technology, Ho Chi Minh City campus. His current research interests include wireless communication, wireless energy harvesting techniques, and the analysis of wireless network performance.

Nguyen Trong KIEN graduated with a Master's degree in Telecommunications Engineering in 2014 from the Posts and Telecommunications Institute of Technology. Received a Doctorate degree in Neuroscience in 2020 in Taiwan. Currently a lecturer in the Department of Electronics Engineering at the Posts and Telecommunications Institute of Technology, based in Ho Chi Minh City. Research areas include non-invasive biosignal processing, embedded system design, biomedical devices.

Tran Trung DUY received the Ph.D degree in electrical engineering from University of Ulsan, South Korea. In 2013, he joined Posts and Telecommunications Institute of Technology, Ho Chi Minh city campus. From 2022, he is an associate Professor of Wireless Communications at PTIT-HCM. His major research interests are cooperative multi-hop, cognitive radio, physical-layer security, energy harvesting, hardware impairments and Fountain codes.

Ngo Hoang AN finished his Engineering degree from the University of Transport and Communications, Vietnam, in 2006. He received his Master of Engineering degree from Ho Chi Minh City University of Technology, Vietnam, in 2011. Now, he is teaching at the Faculty of Electrical and Electronics Engineering, Ho Chi Minh City University of Industry and Trade, Vietnam. Additionally, he is pursuing a Ph.D. at the Industrial University of Ho Chi Minh City, Vietnam. His research interests include cooperative communications, multi-hop relaying, physical-layer security, energy harvesting, short-packet communication, and reconfigurable intelligent surfaces.

Nguyen Tien TUNG received the B.Sc. and M.Sc. degrees from the University of Science Ho Chi Minh City, Vietnam, in 2005 and 2010, respectively, and the Ph.D. degree in electronics from Myongji University, South Korea, in 2021. Since 2011, he has been a Lecturer at the Industrial University of Ho Chi Minh City. His research interests include emerging topics of wireless communication for 5G&6G, including energy harvesting, physical layer security, cognitive radio, non-orthogonal multiple access (NOMA), short-packet communications, the Internet of Things (IoT), and applications of optimization and machine learning for wireless communications.

Anh-Vu LE (corresponding author) is at Communication and Signal Processing Research Group, Faculty of Electrical and Electronics Engineering, Ton Duc Thang University, Ho Chi Minh City, Vietnam. He has been worked as a Postdoc Research Fellow in ROAR Laboratory at Singapore University of Technology and Design. He received his BS in Electronics and Telecommunications from Ha Noi University of Technology, Vietnam and Ph.D. in Electronics and Electrical from the Dongguk University, Korea in 2007 and 2015, respectively. His current research interests include Robotics vision, Robot navigation, Human detection, Action recognition, Feature matching, 3D video processing, Signal processing.